

Solvent isotope effect on the microstructure and
rheology of cationic worm-like micelles near the
isotropic-nematic transition
(Supplementary Information)

Carlos R. López-Barrón* Norman J. Wagner†

May 11, 2011

References

- [1] M. E. Helgeson, M. D. Reichert, Y. T. Hu and N. J. Wagner, *Soft Matter*, 2009, **5**, 3858–3869.
- [2] M. E. Helgeson, P. A. Vasquez, E. W. Kaler and N. J. Wagner, *J. Rheol.*, 2009, **53**, 727–756.
- [3] E. Cappelare, R. Cressely and J. P. Decruppe, *Colloids Surf. A*, 1995, **104**, 353–374.

*Department of Chemical Engineering, University of Delaware, Newark, Delaware 19716, USA

†Department of Chemical Engineering, University of Delaware, Newark, Delaware 19716, USA E-mail: wagnernj@udel.edu

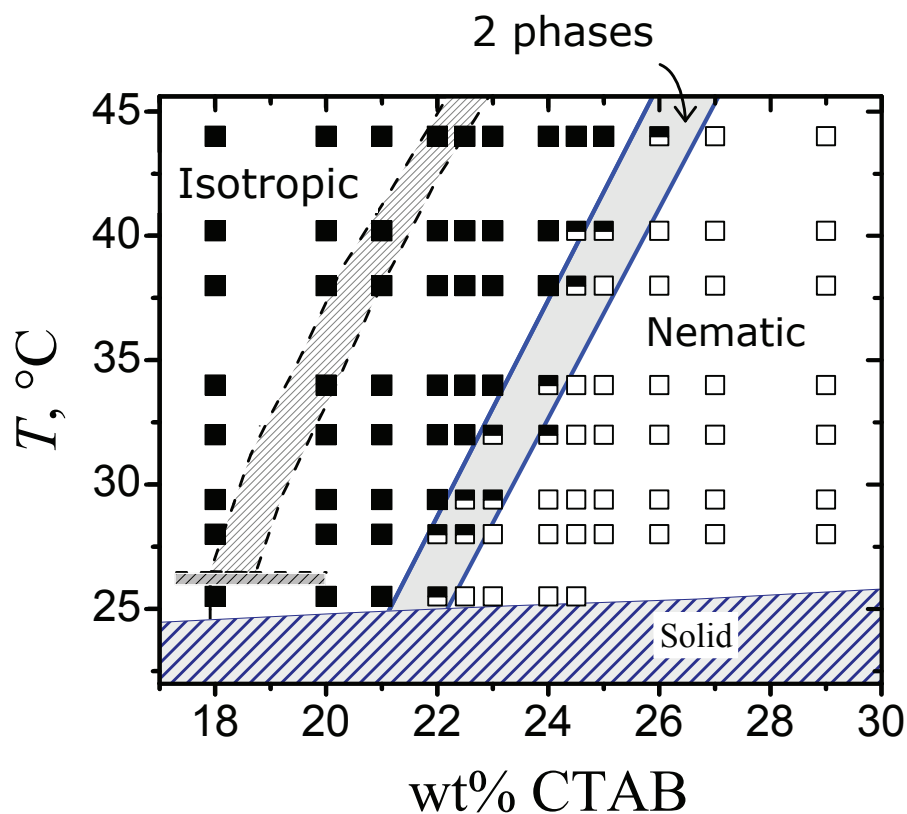


Figure S1. Equilibrium phase diagram of the CTAB/H₂O system obtained using birefringence and flow birefringence observations. Filled symbols, half-filled symbols, and empty symbols represent isotropic, biphasic, and birefringent samples, respectively. Shaded area between dashed lines correspond to the I-N boundary of the CTAB/D₂O system reported in ref. 1. Note: This diagram is equivalent to that shown in Figure 1 (in the paper) where compositions are given in mole fraction. The unit conversion is $y = w / (w + (1 - w)MW_{CTAB}/MW_{H_2O})$ where y and w are mole and weight fractions, respectively, and $MW_{CTAB}=364.45$ g/mol and $MW_{H_2O}=18.02$ g/mol

Table S1. Giesekus model parameters determined from SAOS and steady flow experiments.

CTAB (wt%)	T (°C)	G_0 (Pa)	λ (s)	η_∞ (Pa-s)	α	γ_{1c} (s ⁻¹)	γ_{2c} (s ⁻¹)
20.5	26	103	0.022	0.034	0.871	63	893
	28	148	0.008	0.025	0.818	100	1270
	29	170	0.005	0.023	0.692	251	1585
	30	105	0.007	0.001	0.395	–	–
	32	134	0.003	0.001	0.292	–	–
21.5	30	147	0.009	0.028	0.864	101	1190
	32	199	0.003	0.023	0.803	398	2100
	33	202	0.003	0.010	0.466	–	–
	34	104	0.004	0.003	0.196	–	–
	35	97.8	0.004	0.001	0.077	–	–
22.0	30	68.1	0.041	0.038	0.965	15.8	495
	32	126	0.009	0.032	0.898	63.0	1010
	34	190	0.004	0.025	0.644	251	1570
	35	159	0.004	0.016	0.392	–	–
	40	16	0.010	0.001	0.013	–	–
22.5	34	131	0.010	0.032	0.895	57.4	890
	35	166	0.006	0.027	0.871	158	1370
	36	143	0.006	0.001	0.681	–	–
	37	112	0.006	0.001	0.371	–	–
	40	127	0.002	0.001	0.069	–	–
23.0	35	95.3	0.033	0.035	0.936	39.4	752
	40	96.8	0.004	0.005	0.373	–	–
24.0	40	204	0.004	0.001	0.961	246	1620

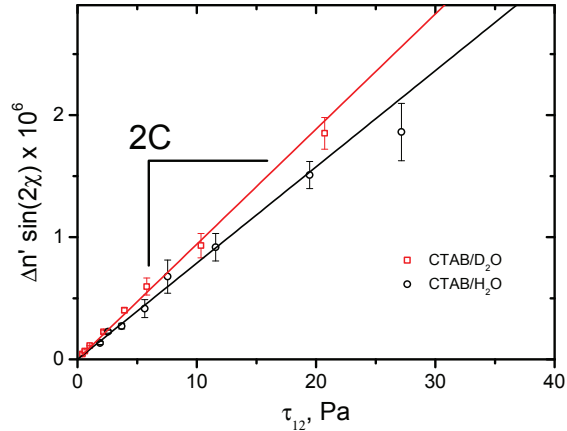


Figure S2. Stress-optic plot for the 22 wt% CTAB/H₂O solution and for the 16.7 wt% CTAB/D₂O solution (after Helgeson et al.²) at 32 °C. Error bars are propagated uncertainties computed with $\delta(\Delta n' \sin 2\chi) = \sqrt{|\sin 2\chi|^2 (\delta \Delta n')^2 + |2\Delta n' \cos 2\chi|^2 (\delta \chi)^2}$.

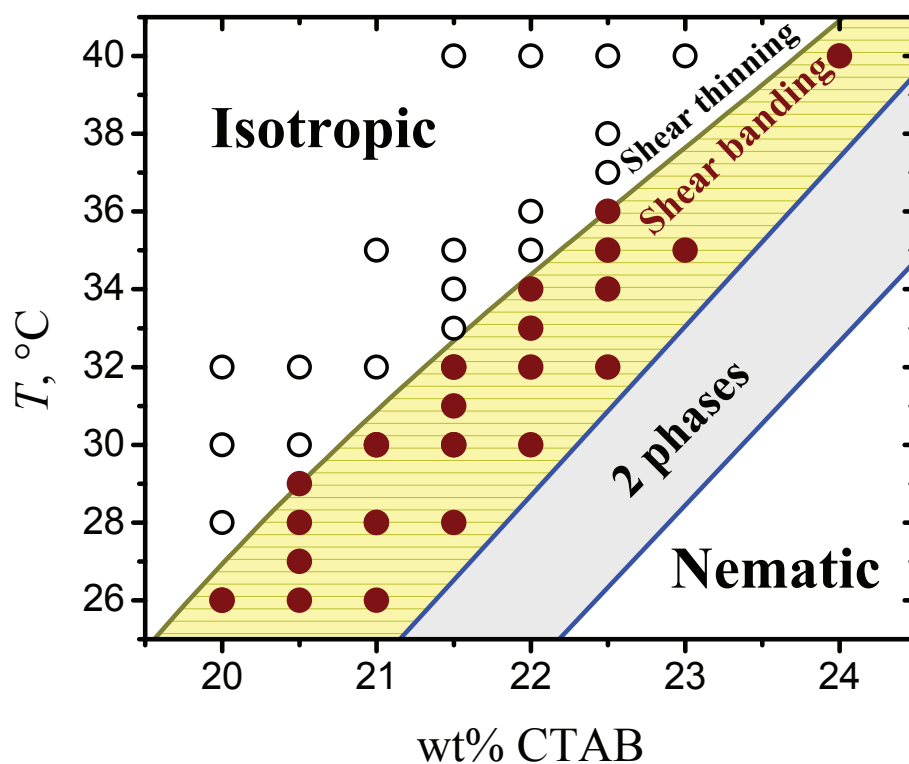


Figure S3. Phase diagram of the CTAB/H₂O system showing the boundary between shear thinning, for which $\alpha < 0.5$ (empty symbols), and shear banding, for which $\alpha \geq 0.5$ (filled symbols). Note: This diagram is equivalent to that shown in Figure 3 (in the paper) where compositions are given in mole fraction. The unit conversion is $y = w / (w + (1 - w)MW_{CTAB}/MW_{H_2O})$ where y and w are mole and weight fractions, respectively, and $MW_{CTAB}=364.45$ g/mol and $MW_{H_2O}=18.02$ g/mol

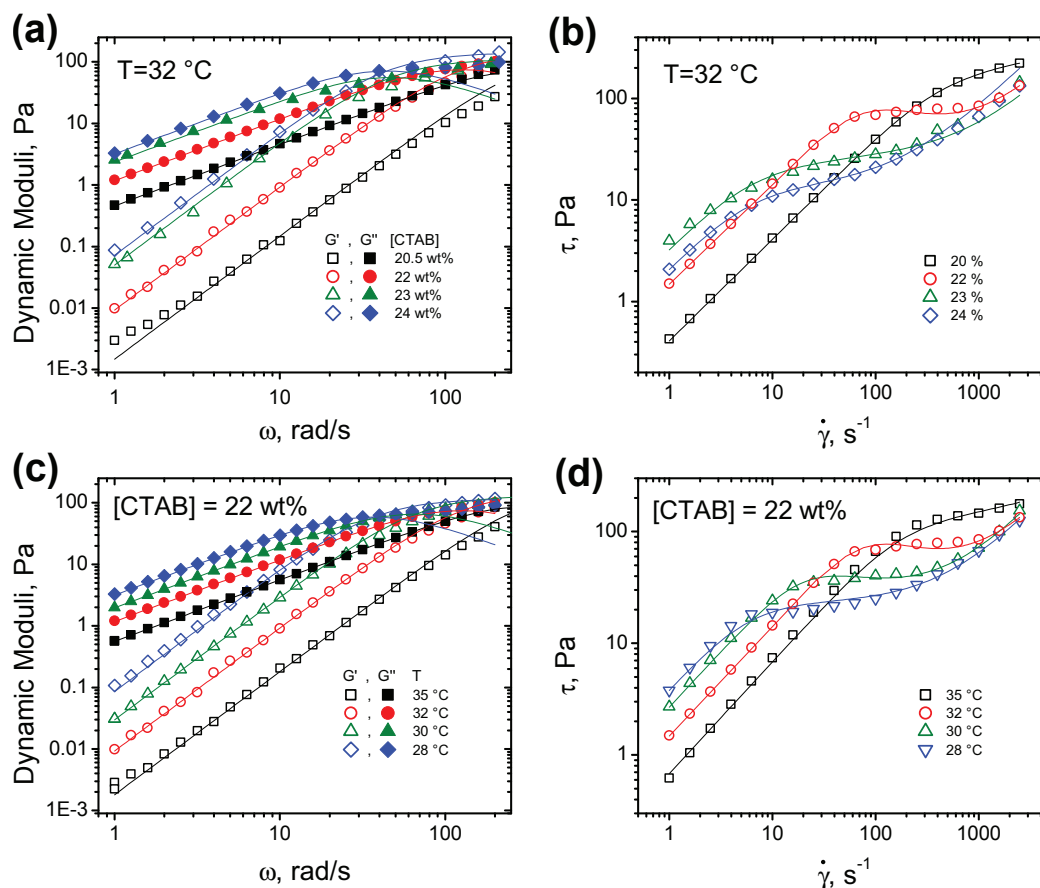


Figure S4. Dynamic frequency sweep (a and c) and steady shear rheology (b and d) for CTAB in H₂O (a and b) at 32 °C with various concentrations spanning the I \ddot{U} N transition and (c and d) for a 22 wt% sample at various temperatures spanning the I \ddot{U} N transition. Points represent experimental data and lines are fits to a single-element Maxwell model with high-frequency viscosity (a and c) and to the Giesekus model under viscometric conditions (b and d).

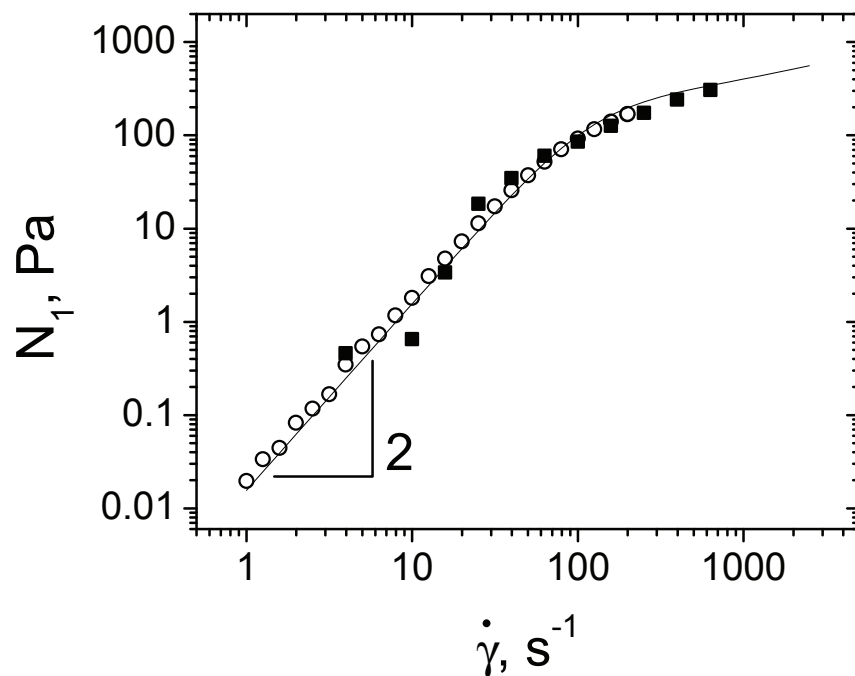


Figure S5. First normal stress difference under steady shear for 22 wt% CTAB in H₂O at 30 °C. Filled symbols represent steady shear measurements on a cone and plate geometry. Data represented by open symbols are calculated from frequency sweep data using the relation $N_1(\dot{\gamma})/\dot{\gamma}^2 = 2G'(\omega)/\omega^2$, which is valid in the viscoelastic linear regime, i.e., at $\omega = \dot{\gamma} \rightarrow 0$. Solid lines give corresponding predictions from the GD model.

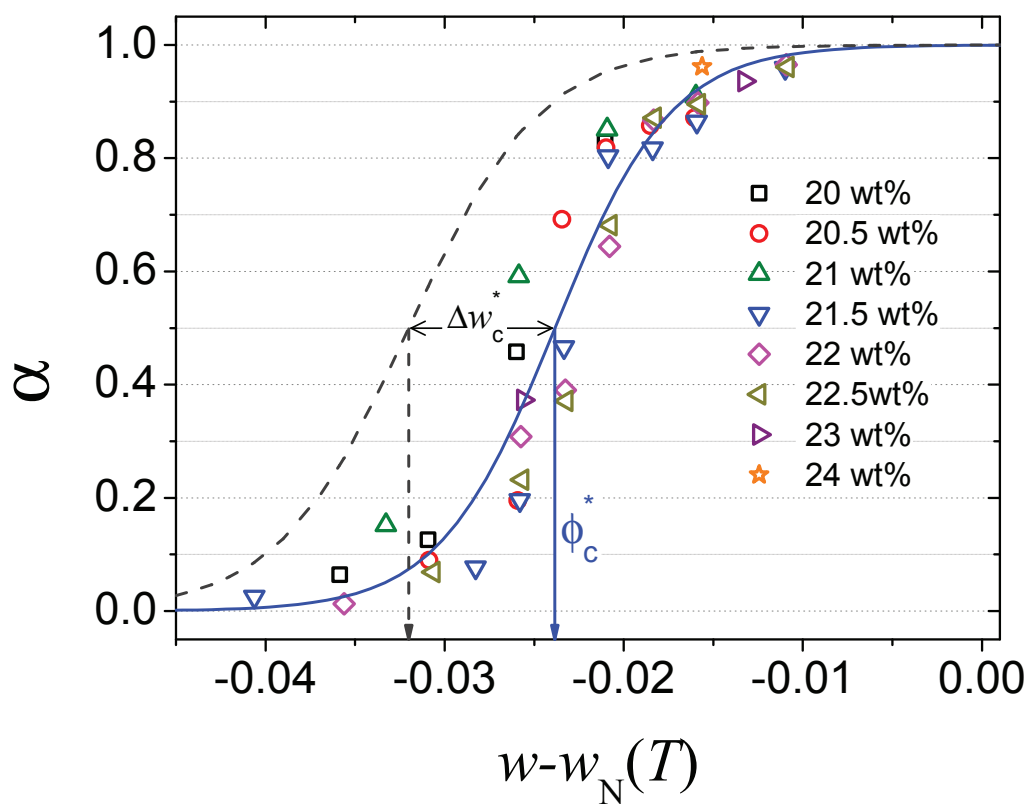


Figure S6. Anisotropy coupling parameter (α) versus compositional order parameter, $w^* = w - w_N$ (Note that Helgeson et al.¹ used the symbol ϕ to denote mass fraction) for all the data point depicted in Fig 3 (in the paper). Solid lines depict the master curves fit with equations 6 and 7. Dashed lines give the fit master curves for the CTAB/D₂O system obtained in ref. 1. Note: This diagram is equivalent to that shown in Figure 6 (in the paper) where compositions are given in mole fraction. The unit conversion is $y = w / (w + (1 - w)MW_{CTAB}/MW_{H_2O})$ where y and w are mole and weight fractions, respectively, and $MW_{CTAB}=364.45$ g/mol and $MW_{H_2O}=18.02$ g/mol

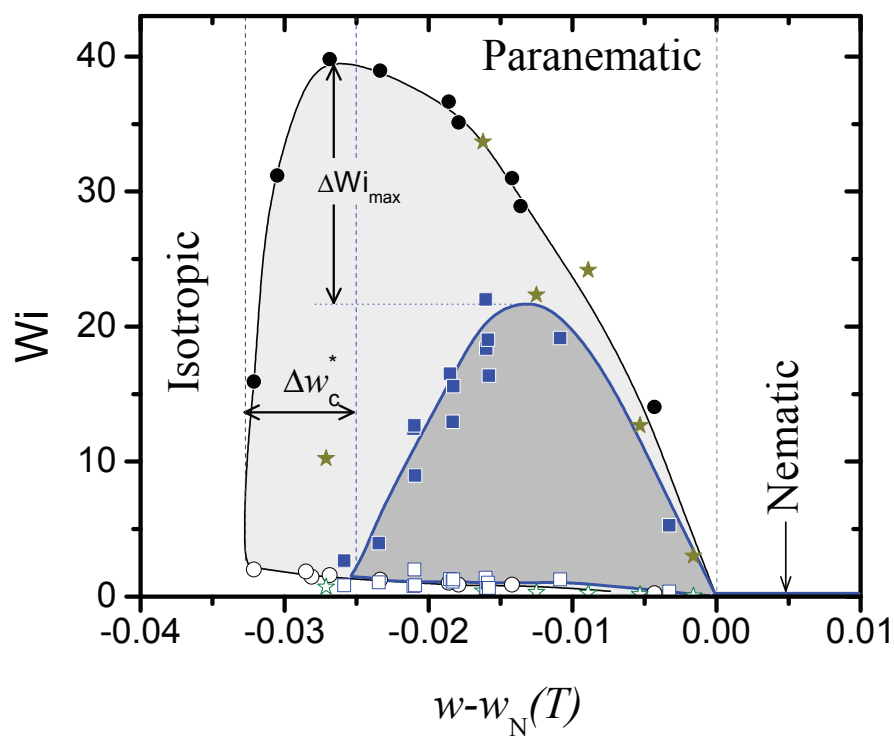


Figure S7. Dimensionless dynamic phase diagram for the systems CTAB/H₂O (squares) and CTAB/D₂O (circles, data reproduced from ref. 1). Triangles depict data for the CTAB/H₂O system taken from ref. 3. Empty and filled symbols represent Wi values corresponding to $\dot{\gamma}_{1c}$ and $\dot{\gamma}_{2c}$, respectively. Note: This diagram is equivalent to that shown in Figure 7 (in the paper) where compositions are given in mole fraction. The unit conversion is $y = w / (w + (1 - w)MW_{CTAB}/MW_{H_2O})$ where y and w are mole and weight fractions, respectively, and $MW_{CTAB}=364.45$ g/mol and $MW_{H_2O}=18.02$ g/mol